Energetics and Dynamics of the Fragmentation Reactions of Protonated Peptides Containing Methionine Sulfoxide or Aspartic Acid via Energy- and Time-Resolved Surface Induced Dissociation

Hadi Lioe,*,†,‡ Julia Laskin,*,§ Gavin E. Reid,∥,⊥ and Richard A. J. O'Hair†,‡,▽

School of Chemistry, University of Melbourne, Victoria 3010, Australia, Bio21 Institute of Molecular Science and Biotechnology, University of Melbourne, Victoria 3010, Australia, Fundamental Science Directorate, Pacific Northwest National Laboratory, Richland, Washington 99352, Department of Chemistry, Michigan State University, East Lansing, Michigan 48824, Department of Biochemistry and Molecular Biology, Michigan State University, East Lansing, Michigan 48824, and ARC Centre of Excellence in Free Radical Chemistry and Biotechnology

Received: April 19, 2007; In Final Form: July 19, 2007

The surface-induced dissociation (SID) of six model peptides containing either methionine sulfoxide or aspartic acid (GAILM(O)GAILR, GAILM(O)GAILK, GAILM(O)GAILA, GAILDGAILR, GAILDGAILK, and GAILDGAILA) have been studied using a specially configured Fourier transform ion-cyclotron resonance mass spectrometer (FT-ICR MS). In particular, we have investigated the energetics and dynamics associated with (i) preferential cleavage of the methionine sulfoxide side chain via the loss of CH_3SOH (64 Da), and (ii) preferential cleavage of the amide bond C-terminal to aspartic acid. The role of proton mobility in these selective bond cleavage reactions was examined by changing the C-terminal residue of the peptide from arginine (nonmobile proton conditions) to lysine (partially mobile proton conditions) to alanine (mobile proton conditions). Time- and energy-resolved fragmentation efficiency curves (TFECs) reveal that selective cleavages due to the methionine sulfoxide and aspartic acid residues are characterized by slow fragmentation kinetics. RRKM modeling of the experimental data suggests that the slow kinetics is associated with large negative entropy effects and these may be due to the presence of rearrangements prior to fragmentation. It was found that the Arrhenius pre-exponential factor (A) for peptide fragmentations occurring via selective bond cleavages are 1−2 orders of magnitude lower than nonselective peptide fragmentation reactions, while the dissociation threshold (E_0) is relatively invariant. This means that selective bond cleavage is kinetically disfavored compared to nonselective amide bond cleavage. It was also found that the energetics and dynamics for the preferential loss of CH_3SOH from peptide ions containing methionine sulfoxide are very similar to selective C-terminal amide bond cleavage at the aspartic acid residue. These results suggest that while preferential cleavage can compete with amide bond cleavage energetically, dynamically, these processes are much slower compared to amide bond cleavage, explaining why these selective bond cleavages are not observed if fragmentation is performed under mobile proton conditions. This study further affirms that fragmentation of peptide ions in the gas phase are predominantly governed by entropic effects.

Introduction

The identification and characterization of post-translational modifications (PTMs) of peptides and proteins remains one of the formidable challenges of tandem mass spectrometry (MS/MS) based proteome analysis techniques,[1,2] especially if the PTM dramatically alters the fragmentation behavior of the peptide ions. One such PTM which changes peptide fragmentation behavior is the commonly observed single oxidation of a methionine residue to methionine sulfoxide. The fragmentation of peptide ions containing methionine sulfoxide is characterized by the preferential diagnostic loss of methane sulfenic acid (CH_3SOH) (64 Da) from the methionine sulfoxide side chain[3] when the number of ionizing protons is less than the number of arginine residues, i.e., under nonmobile proton conditions.[4,5] Previous studies have shown that, under similar conditions of low proton mobility, peptide ions containing aspartic acid residues (and to a lesser extent glutamic acid) undergo preferential backbone cleavage at the peptide bond C-terminal to the acidic amino acid side chain. Selective cleavage at acidic residues often dominates MS/MS spectra and suppresses the intensities of other structurally diagnostic sequence ions in a fashion similar to the preferential loss of CH_3SOH from a methionine sulfoxide residue.[3] Other well-known selective cleavages observed from the fragmentation of protonated peptides under nonmobile proton conditions include peptide bond cleavage C-terminal to oxidized cysteine residue (cysteine sulfinic acid and cysteine sulfonic acid),[6−8] loss of the side chain

* Corresponding authors. Phone: +61 3 8344-2451 (H.L.), (509) 376-4443 (J.L.); Fax: +61 3 9347-5180 (H.L.), (509) 376-6066 (J.L.); E-mail: hlioe@unimelb.edu.au (H.L.), Julia.Laskin@pnl.gov (J.L.).

† School of Chemistry, University of Melbourne.

‡ Bio21 Institute of Molecular Science and Biotechnology, University of Melbourne.

§ Pacific Northwest National Laboratory.

∥ Department of Chemistry, Michigan State University.

⊥ Department of Biochemistry and Molecular Biology, Michigan State University.

▽ ARC Centre of Excellence in Free Radical Chemistry and Biotechnology.

10.1021/jp073040z CCC: $37.00
Published on Web 10/03/2007

SCHEME 1: Mechanism for Preferential Loss of Methane Sulfenic Acid (CH_3SOH) from the Side Chain of Methionine Sulfoxide under Nonmobile Proton Conditions

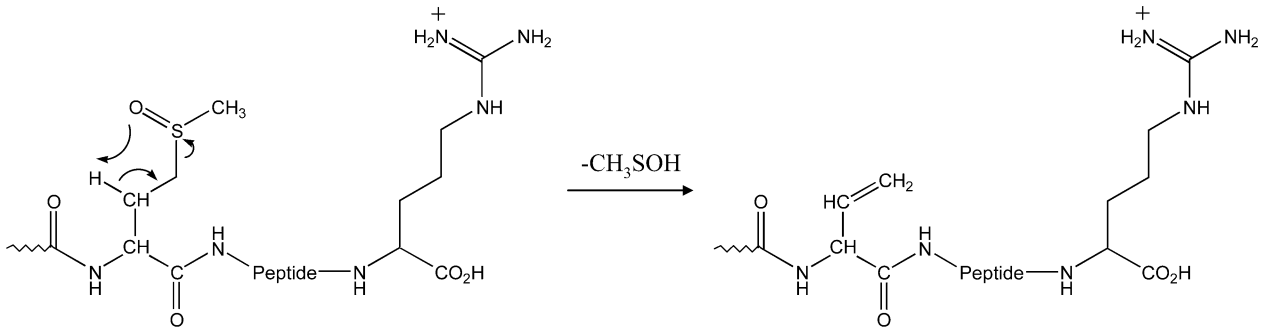

SCHEME 2: Proposed Mechanism for Selective Amide Bond Cleavage C-Terminal to Aspartic Acid under Nonmobile Proton Conditions via (a) Charge Remote cis-1,2-Elimination Mechanism and (b) Salt-Bridge Mechanism

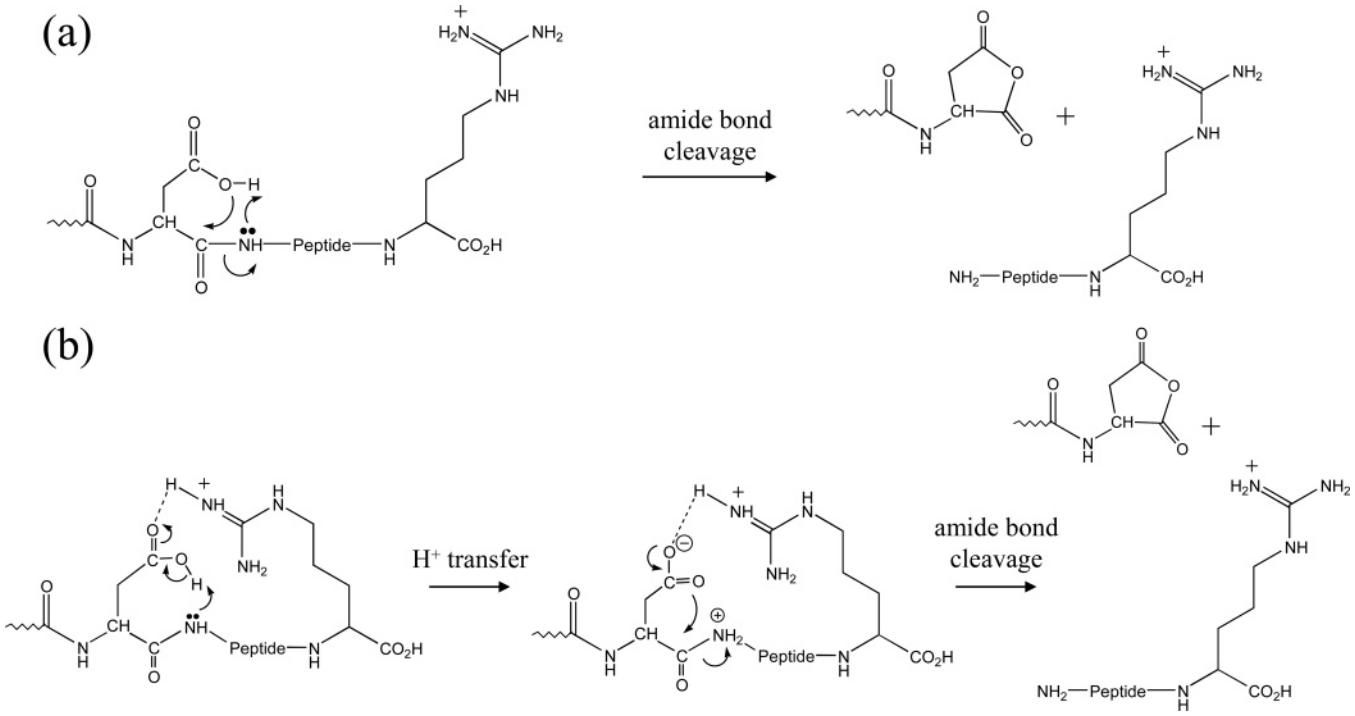

from oxidized *S*-alkyl cysteine residues,[9] and disulfide (S−S and C−S) bond cleavage from cystine moieties.[10]

How do these empirical observations relate to the mechanism(s) of these selective cleavages? The mechanism for CH_3SOH loss from methionine sulfoxide side chains has previously been investigated using a combination of multistage MS^n experiments, isotopic labeling experiments, and molecular orbital calculations.[3,11] It was noted that if the peptide fragments under nonmobile proton conditions, CH_3SOH loss proceeds via a charge remote cis-1,2-elimination mechanism involving concerted abstraction of the β-hydrogen by the moderately basic sulfoxide moiety[12] to form a vinylglycine derivative (Scheme 1). In contrast, if the peptide fragments under mobile proton conditions, loss of CH_3SOH occurs via a charge-directed mechanism involving nucleophilic attack by the amide carbonyl on the N- or C-terminal side of the methionine sulfoxide residue, albeit only at diminished abundance relative to peptide bond cleavage.[3]

Several plausible mechanisms for preferential cleavage of the peptide bond C-terminal to aspartic acid residues have been proposed.[6,13,14] Most of these mechanisms do not directly involve the ionizing charge in the fragmentation process. For example, a charge remote cis-1,2-elimination reaction has been proposed by Tsaprallis et al.[6] (Scheme 2a), where the ionizing proton is sequestered by the arginine residue (R) and where the charge is not solvated and is also not involved in the bond cleavage process. Another charge remote mechanism is shown in Scheme 2b. In this mechanism, the ionizing proton is sequestered at the guanidine side chain of arginine but is solvated by the aspartic acid side chain, which forms a salt-bridge intermediate upon intramolecular proton transfer. This salt-bridge intermediate is then the "reactive geometry" involved in the amide bond cleavage reaction.[14]

A key aspect relevant to the mechanisms of these selective cleavages relates to their energetics and dynamics. Using a specially constructed Fourier transform ion-cyclotron resonance mass spectrometer (FT-ICR MS), the selective dissociation at the aspartic acid residue has previously been investigated via time- and energy-resolved surface induced dissociation (SID) experiments for LDIFSDF, LDIFSDFR, RLDIFSDF, and LEIFSEFR[15] as well as angiotensin analogues (DRVYIHPF, RVYIHPF, RVYIHAF, and RVYIHDF).[16] From RRKM-based

modeling of the time- and energy-resolved fragmentation efficiency curves (TFECs), the dissociation threshold (E_0) for selective fragmentation due to the aspartic acid residue was determined to be very similar to nonselective sequence ion formation. In addition, the RRKM modeling suggests that the Arrhenius pre-exponential factor for Asp cleavage is 2 orders of magnitude smaller than that for nonselective fragmentation; i.e., preferential fragmentations are kinetically disfavored processes, indicative of complex rearrangements taking place preceding selective fragmentation.[15]

Here we report the first comparative study on the energetics and dynamics of two important selective cleavages, CH_3SOH loss from methionine sulfoxide residue versus amide bond cleavage C-terminal to Asp residue, using time- and energy-resolved SID experiments of the model "tryptic" peptides GAILDGAILX and GAILM(O)GAILX, where X = R, K, or A. These peptides were designed to have (1) the same number of amino acid residues, (2) the same sequence except for an internal residue, which is either Asp (D) or methionine sulfoxide (Met(O)), and (3) varying C-terminal residues (arginine (R), lysine (K), or alanine (A)) to manipulate the proton mobility and thus examine how this factor influences the energetics and dynamics of peptide fragmentation.

Experimental Methods

Materials. All peptides GAILDGAILR, GAILDGAILK, GAILDGAILA, GAILMGAILR, GAILMGAILK, and GAILMGAILA were purchased from Auspep (Melbourne, Australia) and were used without further purification. All samples were dissolved in a 70:30 (v/v) methanol:water solution containing 1% acetic acid. A syringe pump (Cole Parmer, Vernon Hills, IL) was used for direct infusion of the electrospray samples at flow rates ranging from 20 to 50 μL/h.

Oxidation of Methionine Derivatives. Lyophilized methionine-containing peptides (1 mg) were dissolved in 50 μL of 50% CH_3OH/50% H_2O containing 0.1 M acetic acid. Then, 50 μL of 30% aqueous hydrogen peroxide was added and the reaction was allowed to proceed at room temperature for 15 min. The mixture was dried and used without further purification. Based on the electrospray ionization/MS precursor ion abundances of the Met(O) derivatives, the reaction had proceeded to near completion (>98%).

Mass Spectrometry Experiments. SID experiments were conducted on a specially designed 6 T Fourier transform ion-cyclotron resonance (FT-ICR) mass spectrometer as described elsewhere.[17] The instrument is equipped with a high-transmission electrospray ionization source, consisting of an ion funnel interface[18] followed by three quadrupoles that provide for pressure drop and ion bunching, mass selection, and ion storage, respectively. The SID target is introduced through a vacuum interlock assembly and is positioned at the rear trapping plate of the ICR cell. Both the instrument and SID experimental protocol have been detailed elsewhere[17] and will be only briefly outlined below.

Ions are electrosprayed at atmospheric pressure into the end of a heated stainless steel capillary tube. The ion funnel that follows the capillary provides highly efficient ion transfer into the high vacuum region of the mass spectrometer. Three quadrupoles following the ion funnel provide collisional focusing, mass selection of the ion of interest, and accumulation of ions external to the ICR cell. Typical accumulation times are in the range of 0.3−0.8 s. The third (accumulation) quadrupole is held at elevated pressure (about 2×10^{-3} Torr) for collisional relaxation of any internal energy possessed by ions generated by electrospray ionization prior to their injection into the ICR cell.

After accumulation, mass-selected ions are extracted from the third quadrupole and transferred into the ICR cell where they collide with the surface. Scattered ions are captured by raising the potentials on the front and rear trapping plates of the ICR cell by 10−20 V. Time-resolved mass spectra were acquired by varying the delay between the gated trapping and the excitation/detection event (the reaction delay). The reaction delay was varied from 1 ms to 1 s. Immediately following the fragmentation delay, ions were excited by a broad-band chirp and detected. The collision energy is defined by the difference in the potential applied to the accumulation quadrupole and the potential applied to the rear trapping plate and the SID target. The ICR cell can be offset above or below ground by as much as ±150 V. Lowering the ICR cell below ground while keeping the potential on the third quadrupole fixed increases collision energy for positive ions.

Experimental control was accomplished with a MIDAS data station.[19] MIDAS is used to control the voltages and timing of the source and transfer optics, as well as ion manipulation in the ICR cell. An automated script was written to allow for unattended acquisition of kinetic data. The script was used to vary the fragmentation delay and collision energy of the experiment. Reactions delays of 1 ms, 5 ms, 10 ms, 50 ms, 0.1 s, and 1 s were studied. Typical experiments involved changing the collision energy across a relatively wide range from 15 to 65 eV. The automated script allowed for acquisition of SID spectra across the entire range of collision energies, in 1 eV increments, at each of the six fragmentation delays. Time-dependent survival curves were constructed from experimental mass spectra by plotting the relative abundance of the precursor ion as a function of collision energy for each delay time.

The self-assembled monolayer (SAM) surface was prepared on a single gold {111} crystal (Monocrystals, Richmond Heights, OH) using a standard procedure. The target was cleaned in a UV cleaner (Model 135500, Boekel Industries Inc., Feasterville, PA) for 10 min and allowed to stand in a 1 mM ethanol solution of FC_{12}, ($CF_3(CF_2)_9C_2H_4SH$), for 24−36 h. The target was removed from the SAM solution and ultrasonically washed in ethanol for 10 min to remove extra layers.

RRKM Modeling. The survival curves (SCs) representing the relative abundance of the parent ion as a function of collision energy were modeled using an RRKM-based approach developed by our group.[20,21] We modeled separately time-dependent (slow) and time-independent (fast) kinetics and used two dissociation rate constants for the total ion decomposition, as indicated schematically below:

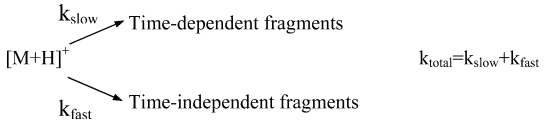

Microcanonical rate constants as a function of internal energy for the slow channel were calculated using RRKM. For the fast reaction pathway the rate−energy dependence is best described by a step function originating at the assumed threshold energy.[22]

Fragmentation probability as a function of the internal energy of the parent ion and the experimental observation time (t_r), $F(E,t_r)$, is given by

$$F(E,t_r) = e^{-(k_{total})(E)+(k_{rad})t_r} \quad (1)$$

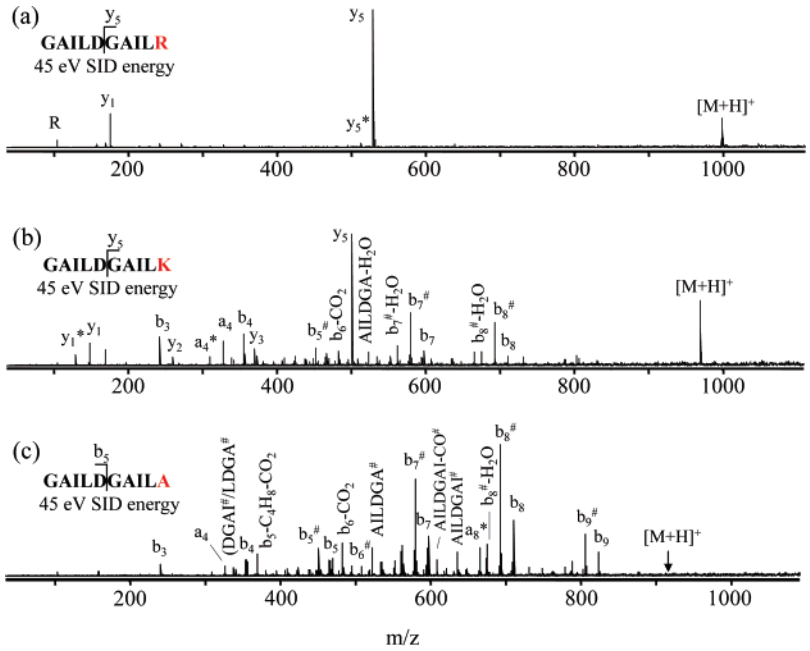

Figure 1. SID MS/MS product ion spectra of singly protonated model peptide ions containing aspartic acid as a function of proton mobility: (a) GAILDGAILR, (b) GAILDGAILK, and (c) GAILDGAILA at 45 eV collision energy. SID experiments were performed using FSAM surface as target and with reaction delays of 1.0 s. The $\mathbf{b}_n$-H_2O and $\mathbf{a}_n$-NH_3 ions are represented by $\mathbf{b}_n^{\#}$ and $\mathbf{a}_n$*, respectively.

where k_{rad} is the rate constant for radiative cooling of the excited ion. A breakdown graph for dissociation of the parent ion into several fragments was constructed using formal kinetics equations corresponding to a specific reaction scheme.

The energy deposition function was described by the following analytical expression:

$$P(E,E_{coll}) = \frac{(E-\Delta)^l}{C}\exp\left(-\frac{E-\Delta}{f(E_{coll})}\right) \quad (2)$$

where l and Δ are parameters, $C = \Gamma(l+1)[f(E_{coll})]^{l+1}$ is a normalization factor, and $f(E_{coll})$ has the form

$$f(E_{coll}) = A_2E_{coll}^{\ 2} + A_1E_{coll} + A_0 \quad (3)$$

where A_0, A_1, and A_2 are parameters, and E_{coll} is the collision energy. Finally, the normalized signal intensity for a particular reaction channel is given by the equation

$$I_i(E_{coll}) = \int_0^\infty F_i(E,t_r)\,P(E,E_{coll})\,dE \quad (4)$$

Time- and collision-energy-resolved SCs or fragmentation efficiency curves (TFECs) for different fragments were constructed using the above procedure and compared to experimental data. The energy deposition function was kept the same for all reaction times. Fitting parameters were varied until the best fit to experimental curves was obtained. These parameters included the critical energy and the activation entropy for the total decomposition of the precursor ion, the threshold for the fast fragmentation, and parameters characterizing the energy deposition function (eqs 2 and 3). The uniqueness of the fits was confirmed using sensitivity analysis described previously.[21]

Vibrational frequencies of precursor ions were obtained from the frequency model given by Christie and co-workers.[23] Vibrational frequencies for the transition states were estimated by removing one C−N stretch (reaction coordinate) from the parent ion frequencies and varying all frequencies in the range of 500−1000 cm^{-1} to obtain the best fit with experimental data.

Results and Discussion

Fragmentation Reactions of Protonated Peptides Containing Aspartic Acid and Methionine Sulfoxide Residue. As it had previously been demonstrated that preferential cleavage due to aspartic acid[15] and methionine sulfoxide residues[3] are highly dependent on proton mobility, we have examined the energetics and dynamics for these selective fragmentation reactions of singly protonated model peptides under various proton mobility conditions: GAILDGAILA and GAILM(O)GAILA, which fragment under mobile proton conditions due to the absence of any basic amino acid residues; GAILDGAILK and GAILM(O)GAILK, which fragment under partial mobile proton conditions due to the presence of the moderately basic amino acid, lysine (K); and GAILDGAILR and GAILM(O)GAILR, which fragment under nonmobile proton conditions due to the presence of the highly basic amino acid, arginine (R).

Figure 1 shows the SID spectra of singly protonated peptides containing aspartic acid GAILDGAILR (Figure 1a), GAILDGAILK (Figure 1b), and GAILDGAILA (Figure 1c) at a collision energy of 45.0 eV using a fluorinated self-assembled monolayer (FSAM) surface and a reaction delay of 1.0 s. The spectrum for GAILDGAILR is characterized by the almost exclusive formation of the $\mathbf{y}_5$ ion due to selective amide bond cleavage C-terminal to the aspartic acid (D) residue. Other fragments observed for this peptide include the $\mathbf{y}_5$-NH_3, $\mathbf{y}_1$, and the immonium ion of arginine (R). Note that only **y**-type ions are formed due to the proton being sequestered at the C-terminal arginine residue. This result is consistent with previous work, which demonstrated that the preferential amide bond cleavage due to aspartic acid residue can dominate the fragmentation when the experiment is performed under nonmobile proton conditions.[6,15]

Amide bond cleavage C-terminal to the aspartic acid (D) still dominates the spectrum when the C-terminal amino acid residue is substituted with lysine (K) (Figure 1b). However, many

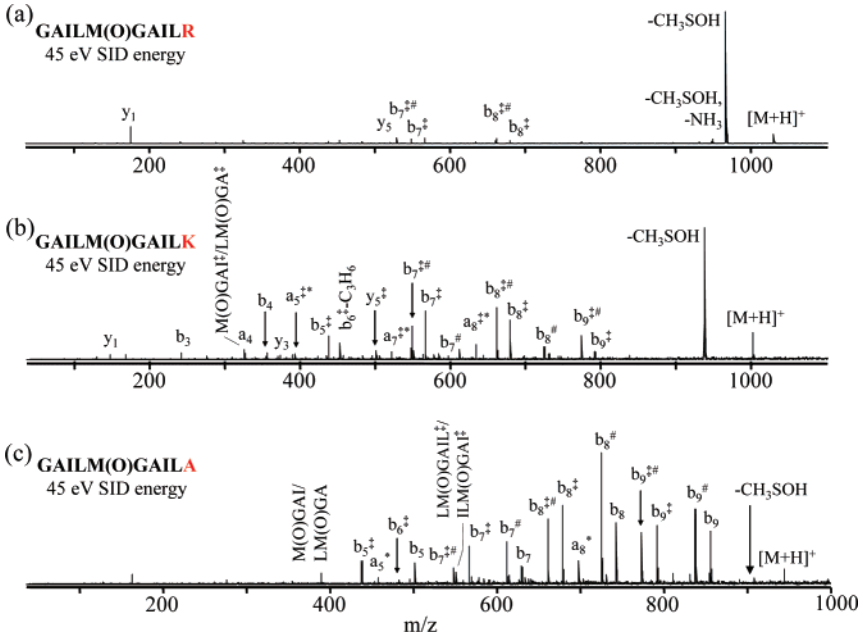

Figure 2. SID MS/MS product ion spectra of singly protonated model peptide ions containing methionine sulfoxide as a function of proton mobility: (a) GAILM(O)GAILR, (b) GAILM(O)GAILK, and (c) GAILM(O)GAILA at 45 eV collision energy. SID experiments were performed using FSAM surface as target and with reaction delay of 1.0 s. The $\mathbf{b}_n$-H_2O, $\mathbf{a}_n$-NH_3, $\mathbf{b}_n$-CH_3SOH, $\mathbf{b}_n$-CH_3SOH-H_2O, and $\mathbf{a}_n$-CH_3SOH-NH_3 ions are represented by $\mathbf{b}_n^{\#}$, $\mathbf{a}_n$*, $\mathbf{b}_n^{\ddagger}$, $\mathbf{b}_n^{\ddagger\#}$, and $\mathbf{a}_n^{\ddagger}$*, respectively.

additional sequence ions are also observed in the spectrum. The SID spectrum of GAILDGAILK appears to be the intermediate case of the two extremes: GAILDGAILR, which fragments selectively, and GAILDGAILA, which fragments nonselectively. This therefore suggests that nonselective amide bond cleavage competes with selective cleavage at aspartic acid for this peptide. Furthermore, more N-terminal **b**-type fragment ions ($\mathbf{b}_n$, n = 3−8) are observed in the fragmentation of GAILDGAILK due to the reduced basicity of lysine. Some $\mathbf{b}_n$-H_2O ions are also observed (labeled as $\mathbf{b}_n^{\#}$ ions). When the nonbasic alanine (A) residue is at the C-terminus, very little selective aspartic acid (D) amide bond cleavage ($\mathbf{b}_5$ ion) is observed in the MS/MS spectrum (Figure 1c). Instead, the spectrum is dominated by $\mathbf{b}_n$, $\mathbf{b}_n$-H_2O, $\mathbf{a}_n$, $\mathbf{a}_n$-NH_3, and internal **b** (note that $\mathbf{a}_n$-NH_3 ions are labeled as $\mathbf{a}_n$*) sequence ions. From the extensive series of **b** ions formed, the identity of the peptide can easily be determined.

Similar fragmentation behavior is observed from the product ion spectra of singly protonated peptides containing methionine sulfoxide GAILM(O)GAILR (Figure 2a), GAILM(O)GAILK (Figure 2b), and GAILM(O)GAILA (Figure 2c), obtained at collision energies of 45.0 eV using the FSAM surface and a reaction delay of 1.0 s. For GAILM(O)GAILR, the almost exclusive loss of methane sulfenic acid (CH_3SOH, 64 Da) is observed, due to the proton being sequestered at the C-terminal arginine (R) residue (nonmobile proton conditions). As previously mentioned, this diagnostic CH_3SOH loss has been demonstrated to occur by a charge remote process, i.e., the ionizing proton is not involved in dissociation,[3] and hence is consistent with CH_3SOH loss being capable of dominating the fragmentation even in the absence of a mobile proton. A small abundance of $\mathbf{y}_1$ and $\mathbf{y}_5$ ions are also formed, and interestingly $\mathbf{b}_n$-CH_3SOH and $\mathbf{b}_n$-CH_3SOH-H_2O ions (for n = 7,8) are also observed (these $\mathbf{b}_n$-CH_3SOH and $\mathbf{b}_n$-CH_3SOH-H_2O ions are labeled as $\mathbf{b}_n^{\ddagger}$ and $\mathbf{b}_n^{\ddagger\#}$, respectively). The latter two product ions are most likely formed by consecutive fragmentation of the $[M + H - CH_3SOH]^+$ ion.

For the $[M + H]^+$ precursor ion of GAILM(O)GAILK, where fragmentation occurs under partial mobile proton conditions (Figure 2b), the product ion spectrum is still dominated by the loss of CH_3SOH from the precursor ion. In addition, product ions corresponding to subsequent fragmentation of the $[M + H - CH_3SOH]^+$ ion are also observed (the $\mathbf{a}_n$-CH_3SOH-NH_3, $\mathbf{b}_n$-CH_3SOH, and $\mathbf{b}_n$-CH_3SOH-H_2O ions, labeled as $\mathbf{a}_n^{\ddagger}$*, $\mathbf{b}_n^{\ddagger}$, and $\mathbf{b}_n^{\ddagger\#}$, respectively). Sequence ions are also formed directly from the $[M + H]^+$ of GAILM(O)GAILK, including the $\mathbf{a}_n$, $\mathbf{b}_n$, and $\mathbf{b}_n$-H_2O (n = 3, 4, 7 and 8). This result demonstrates that partial sequestration of the proton not only affects the initial proton mobility during dissociation of the peptide ion, but also influences the proton mobility of the fragment ion. Therefore, when fragmentation occurs under partial proton mobility, the ionizing proton is only partially sequestered at the basic residue to sample more sites and increase the probability for the formation of sequence ions directly from the precursor ion and also from the $[M + H - CH_3SOH]^+$ product ion. When the C-terminal residue is substituted with the nonbasic alanine (A) residue, abundant sequence ions are formed, including $\mathbf{b}_n$, $\mathbf{b}_n$-H_2O, and $\mathbf{a}_n$-NH_3, (n = 5, 7, 8, and 9) as shown in Figure 2c for GAILM(O)GAILA. Remarkably, a low abundance product ion corresponding to CH_3SOH loss is observed. The presence of abundant products corresponding to subsequent fragmentation of the $[M + H - CH_3SOH]^+$ ion (e.g., $\mathbf{b}_n$-CH_3SOH and $\mathbf{b}_n$-CH_3SOH-H_2O ions) suggest that the initially formed $[M + H - CH_3SOH]^+$ ion is fairly unstable and readily fragments on the time scale of the experiment. Note that only N-terminal product ions are formed from fragmentation of GAILM(O)GAILA, due to a lack of a basic residue on the C-terminal side of the peptide.

These results suggest the following: (i) if fragmentation of protonated peptides containing methionine sulfoxide occurs under nonmobile proton conditions, the diagnostic loss of CH_3SOH can dominate the MS/MS spectrum, limiting the ability to subsequently determine the sequence of the peptide; (ii) if fragmentation occurs under mobile proton conditions, abundant

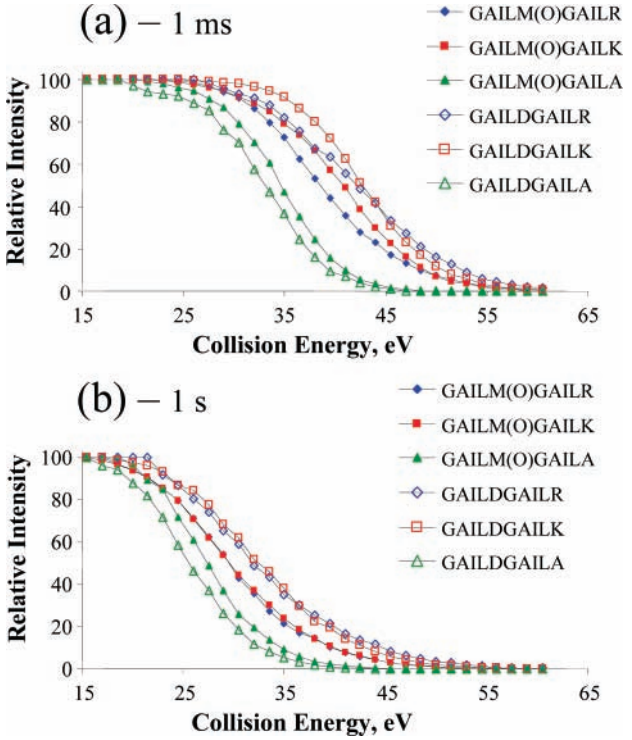

Figure 3. Comparison of survival curves of parent ions for all peptides studied at (a) 1 ms and (b) 1 s reaction delays.

sequence ions are formed, together with the formation of sequence ions arising from subsequent fragmentation from the $[M + H - CH_3SOH]^+$ ion, thus further enhancing the ability to identify the peptide. Similar formation of $\mathbf{b}_n$-CH_3SOH fragment ions have been reported.[24] Consistent with previous reports, it is also noteworthy that the selective dissociation due to aspartic acid and methionine sulfoxide residues at different proton mobility conditions are very similar.[3]

Energy-Resolved Survival Curves (SCs). The advantage of performing SID experiment in an ion-trapping instrument is that reaction can be monitored as a function of time (reaction delay) so that product ions formed by fast and slow dissociation processes can be observed. The stability of the precursor ions of different peptides can also be studied and compared at various reaction delays. Collision-energy-resolved survival curves (SCs) of all peptides obtained at 1 ms and 1 s reaction delays are shown in parts a and b, respectively, of Figure 3. The SC represents the relative abundance of the unfragmented precursor ion as a function of collision energy. Generally, more energy is required to dissociate the precursor ion at shorter reaction delay. For example, the 30 eV onset of fragmentation for GAILDGAILK at the shortest reaction delay of 1 ms is significantly higher than the 20 eV onset at the 1 s reaction delay. This observation is common for the fragmentation of large precursor ions[25] and is attributed to the reduced kinetic shift at longer reaction delays.[26]

For all peptides studied, the nonbasic peptides GAILM(O)-GAILA and GAILDGAILA required lower energies for dissociation. The GAILDGAILK peptide, on the other hand, appears to be the most stable peptide in the series of peptides studied with the SC shifted to higher energies at 1 ms reaction delay. For peptides that fragment by selective or partially selective dissociation, it is noted that GAILM(O)GAILR and GAILM(O)GAILK require lower energy for dissociation than the corresponding Asp-containing peptides. However, it is also of interest to note that the SCs of GAILDGAILR and GAILD-GAILK, and of GAILM(O)GAILR and GAILM(O)GAILK,

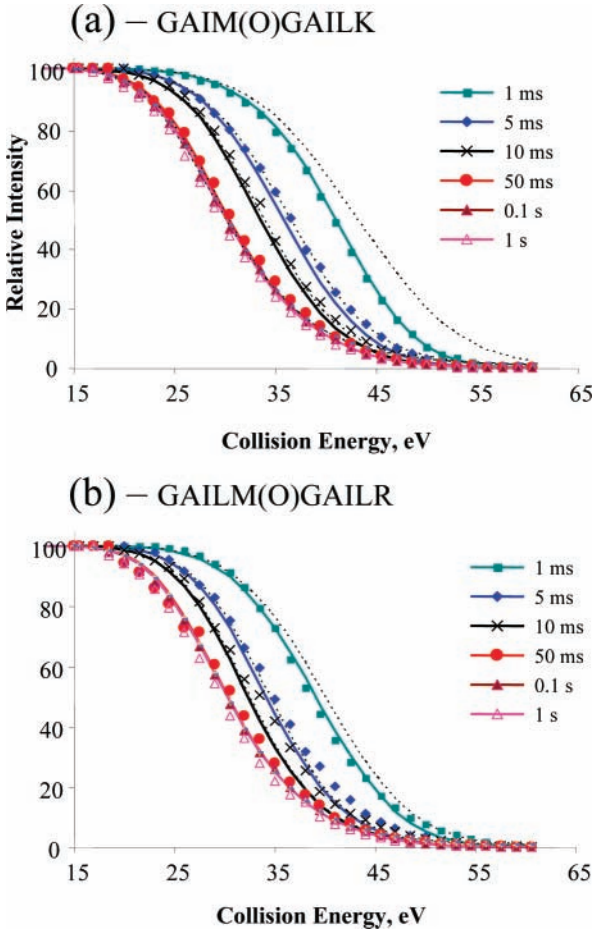

Figure 4. Time- and energy-resolved fragmentation efficiency curves (TFECs) for (a) GAILM(O)GAILK and (b) GAILM(O)GAILR at 1 ms, 5 ms, 10 ms, 50 ms, 0.1 s, and 1 s. Also included in the figures are the RRKM-based modeling fit to the experimental time-resolved fragmentation efficiency curves. The experimental TFECs at various reaction delays are shown by the points, while the modeling fit to the experimental data is represented by the lines. Dotted lines (···) represent modeling of the experimental TFEC without any contribution from fast fragmentation.

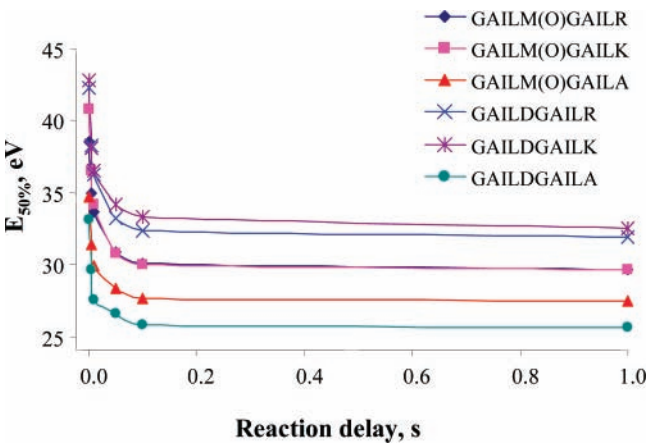

Figure 5. $E_{50\%}$ (collision energy required to observe 50% fragmentation of the precursor ion) of all peptides studied as a function of reaction delay.

nearly coincide at 1 s of reaction delay. The SCs of these peptides are characterized by not only the change in onset for dissociation as the reaction delay is changed from 1 ms to 1 s, but also the relative position of the curves and the shape of the SCs, indicating differences in entropy effects in dissociation.

TABLE 1: Results of the RRKM Modeling of the Experimental Time- and Energy-Resolved Fragmentation Efficiency Curves[a]

	GAILDGAILA	GAILDGAILK	GAILDGAILR	GAILM(O)GAILA	GAILM(O)GAILK	GAILM(O)GAILR
E_0 (eV)	1.27	1.28	1.33	1.33	1.15	1.20
ΔS (cal mol^{-1} K^{-1})	−7.0	−12.9	−11.5	−3.1	−14.5	−12.3
A (s^{-1})	7.7×10^{11}	3.8×10^{10}	8.0×10^{10}	5.4×10^{12}	1.8×10^{10}	5.3×10^{10}
E_{fast} (eV)	10.4	10.4	10.4	9.2	10.6	10.8

[a] E_0 is the threshold energy, $\Delta S^{\ddagger}$ is the entropy change for the transition state, A is the pre-exponential factor at 450 K, and E_{fast} is the threshold energy for shattering.

It has previously been shown that the shapes of SCs are characteristic of the reaction entropy.[16] Kinetically unfavored reactions with large negative reaction entropies are associated with shallow SCs, while fast (kinetically favored) fragmentation results in steep SCs. Interestingly, the SCs of the nonbasic peptides (GAILM(O)GAILA and GAILDGAILA) are steeper than the basic peptides, suggesting that dissociations of these peptides are kinetically favored. This is consistent with previous studies showing that formation of sequence ions via nonselective fragmentations are characterized by significantly faster kinetics than selective fragmentation.[15,16]

The time- and energy-resolved SCs for GAILM(O)GAILK and GAILM(O)GAILR obtained at various reaction delays (1 ms, 5 ms, 10 ms, 50 ms, 0.1 s, and 1 s) are shown in parts a and b, respectively, of Figure 4. As expected, the dissociation of both GAILM(O)GAILK and GAILM(O)GAILR at 1 ms requires higher energy than at longer reaction delay due to the kinetic shift. However, the energy required to fragment both peptides seems to be constant after 50 ms of reaction delay. This is further illustrated in Figure 5, which shows the collision energy required to fragment 50% of the precursor ion ($E_{50\%}$) as a function of reaction delays for the $[M + H]^+$ ions of all peptides studied. The $E_{50\%}$ values of all peptides are characterized by a dramatic decrease as the reaction time is increased from 1 ms to 0.1 s, but then tail off after 0.1 s. This leveling of the $E_{50\%}$ results from the competition between the unimolecular dissociation and the radiative cooling of the vibrationally excited precursor ion, which becomes a dominant process at long reaction delays. It is interesting to note that while at 1 ms reaction delay the $E_{50\%}$ of GAILM(O)GAILR is lower than the $E_{50\%}$ of GAILM(O)GAILK they perfectly overlap at the longer reaction delay. The decreases in the $E_{50\%}$ values of GAILM(O)GAILR, GAILM(O)GAILK, GAILM(O)GAILA, GAILDGAILR, GAILDGAILK, and GAILDGAILA as the reaction delay was increased from 1 ms to 1 s were determined to be 9.0, 11.2, 7.3, 10.3, 10.2, and 7.5 eV, respectively. From Figure 5 it was also observed that the nonbasic peptides (GAILM(O)GAILA and GAILDGAILA) were the least stable toward fragmentation, and consistent with the energy-resolved SCs (Figure 3a), GAILDGAILK is the most stable peptide toward dissociation.

RRKM Modeling of the Time-Resolved Survival Curves. Modeling of the experimental time- and energy-resolved SCs using the RRKM-based approach outlined in the experimental section provided further insights into the energetics and dynamics of dissociation, and the modeling parameters can be compared for different peptides. The results of RRKM-based modeling of the experimental SCs for GAILM(O)GAILK and GAILM(O)GAILR at various reaction delays are also shown in parts a and b, respectively, of Figure 4. Dotted lines in Figure 4 show only the contribution of slow fragmentation to the SCs. The larger deviation between the experimental SCs and the dotted lines indicates that the fragmentation of these peptides has greater contribution from the fast (shattering) component.[22] From Figure 4, it is clear that GAILM(O)GAILK has greater contribution from fast decay than GAILM(O)GAILR. This contribution of the fast decay is known to affect the shape of the SC at the short reaction delay, and in the case of GAILM(O)GAILK this is characterized by a steep SC at 1 ms reaction delay (see Figure 3a).

It should be noted that, according to our time- and energy-resolved SID spectra for the lysine (K) containing peptides, selective cleavage accounts for 60−80% fragmentation of the precursor ion over a broad range of collision energies (data not shown). This suggests that the dissociation rate (see below) obtained for lysine containing peptides mainly reflects the rate of selective fragmentation. At higher collision energy nonspecific cleavages become important but do not have a significant effect on the relative stability of the $[M + H]^+$ ion. Nevertheless, they are very important for obtaining good sequence information.

The dissociation parameters obtained from the RRKM modeling of SCs of all peptide ions studied are shown in Table 1. The dissociation threshold (E_0) of 1.15 eV was obtained for GAILM(O)GAILK. Substituting the C-terminal amino acid with arginine (R) increases the dissociation threshold (E_0) by 0.05 eV (Table 1). While this increase in dissociation threshold (E_0) is very small, it can still be measured in our instrument. Interestingly, the highest dissociation threshold (E_0) was observed for GAILM(O)GAILA, which fragments nonselectively. It is important to emphasize that the relative stabilities observed experimentally do not necessarily reflect the relative values of dissociation thresholds. The relative stabilities reflect a combination of the energetic and entropic effects (see below), which can compensate one another. Reaction with high dissociation threshold may have a faster experimental rate constant if the activation entropy for the reaction makes it kinetically favorable.

Very similar dissociation thresholds were obtained for all the peptides containing aspartic acid residues. The dissociation threshold for GAILDGAILK is 1.28 eV, which is 0.13 eV higher than the value obtained for its methionine sulfoxide counterpart. A similar small increase in the dissociation threshold (from 1.28 to 1.33 eV) was also observed when the C-terminal amino acid was substituted from the moderately basic lysine (K) to the highly basic arginine (R). However, in contrast to the result obtained for the methionine sulfoxide peptides, the dissociation threshold for the nonbasic GAILDGAILA (1.27 eV) is very similar to the dissociation threshold of GAILDGAILK (Table 1). Both the absolute values and the relative trends in dissociation thresholds for peptides containing aspartic acid are consistent with previously reported results.[15] It is interesting to note that even though there are some small differences in the dissociation thresholds (E_0) for fragmentation of peptides containing aspartic acid (D) or methionine sulfoxide (M(O)) residues under different proton mobility conditions, the difference in the dissociation threshold (E_0) for all peptides studied is in fact relatively small, but significant (maximum $\Delta E_0 = 0.18$ eV).

Another equally important parameter in determining the relative stability of peptide ions toward dissociation is the kinetics of dissociation, which is characterized by the activation entropy or the Arrhenius pre-exponential factor (A). When the results of dissociation threshold (E_0) are combined with the

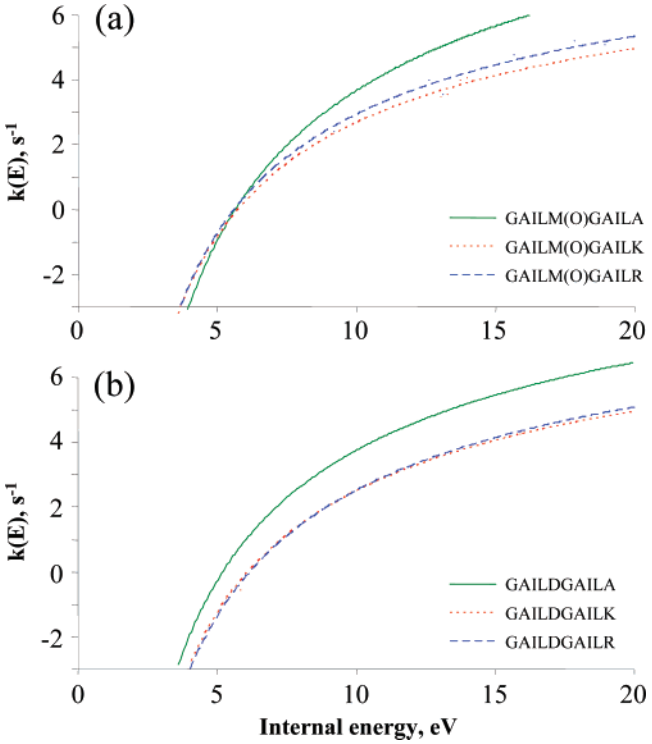

Figure 6. Microcanonical rate energy dependencies for (a) peptides containing methionine sulfoxide residue, GAILM(O)GAILA, GAILM(O)GAILK, GAILM(O)GAILR; and (b) peptides containing aspartic acid residue, GAILDGAILA, GAILDGAILK, GAILDGAILR.

Arrhenius pre-exponential factor, an energy-dependent microcanonical RRKM rate constant can be determined for each peptide studied. Figure 6a shows the microcanonical rate constants as a function of internal energy for the $[M + H]^+$ ions of GAILM(O)GAILA, GAILM(O)GAILK, and GAILM(O)GAILR, while those for the $[M + H]^+$ ions of GAILDGAILA, GAILDGAILK, and GAILDGAILR are shown in Figure 6b.

The Arrhenius pre-exponential factor for dissociation of GAILM(O)GAILA is 5.4×10^{12} s^{-1}, which is 2 orders of magnitude higher than the pre-exponential factor obtained for the more basic analogue GAILM(O)GAILR ($A = 5.3 \times 10^{10}$ s^{-1}) and 300 times higher than the pre-exponential factor obtained for GAILM(O)GAILK ($A = 1.8 \times 10^{10}$ s^{-1}). Similarly, the pre-exponential factor for GAILDGAILA (7.7×10^{11} s^{-1}) is an order of magnitude higher than the *A*-factor for GAILDGAILR (8.0×10^{10} s^{-1}) and 20 times higher than the *A*-factor for GAILDGAILK (3.8×10^{10} s^{-1}). These results demonstrate that the nonselective fragmentation is kinetically favored compared to the selective fragmentation. This behavior is also reflected in the energy-dependent RRKM rate constant, which rises very quickly with increasing internal energy for GAILM(O)GAILA and GAILDGAILA compared to the microcanonical rate constants obtained for selective fragmentation (see Figure 6 for the microcanonical RRKM rate constants of GAILDGAILA and GAILM(O)GAILA). Thus, on the time scale of a trapping instrument, such as an FT-ICR MS, these two nonbasic peptides are least stable toward fragmentation.

While the dissociation threshold for GAILM(O)GAILA is higher than the threshold energies of the corresponding lysine- and arginine-containing peptides, the much larger activation entropy observed for GAILM(O)GAILA causes its microcanonical rate constant to increase much faster with internal energy than the microcanonical rate constants of the lysine- and arginine-containing peptides. As a result, the $k(E)$ curves cross at the internal energy of ca. 5.5 eV, corresponding to experimental rate constant of ca. 1 s^{-1}. It follows that, at internal energies above 5.5 eV, nonselective fragmentation of GAILM(O)GAILA is always faster than selective fragmentation of GAILM(O)GAILK and GAILM(O)GAILR.

The observation that selective fragmentation of the aspartic acid containing peptides are kinetically disfavored are consistent with a previous study,[15] which demonstrated a dramatic decrease in the Arrhenius pre-exponential factor (*A*) by 2 orders of magnitude for the transition from selective to nonselective fragmentation. Interestingly, the present study also demonstrates that selective fragmentation due to methionine sulfoxide follows a similar trend of being kinetically disfavored. It should be noted that substituting the C-terminal arginine (R) residue with lysine (K) alters the kinetics of the fragmentation. For example, the pre-exponential factor of GAILM(O)GAILK (1.8×10^{10} s^{-1}) is 3 times smaller than that of GAILM(O)GAILR (5.3×10^{10} s^{-1}) and that of GAILDGAILK (3.8×10^{10} s^{-1}) is 2 times smaller than that of GAILDGAILR (8.0×10^{10} s^{-1}). Thus, the fragmentation of both peptides under partial proton mobility also suffers from entropic effects. The microcanonical rate−energy dependencies of these lysine-containing moderately basic peptides show behavior similar to that of the basic peptides with the rate constant increasing slowly as the internal energy of the precursor ion increases; thus these peptides are stable toward dissociation (Figure 6).

Conclusions

By using the powerful combination of rationally designed peptides and the unique capabilities of a SID FT-ICR mass spectrometer, we have been able to further shed light on important aspects of the energetics and dynamics of two key selective cleavages. First, this study further highlights the role of proton mobility in the fragmentation of protonated peptides containing aspartic acid or methionine sulfoxide under SID conditions. Under nonmobile proton conditions, the fragmentation of protonated GAILDGAILR is dominated by the formation of a $\mathbf{y}_5$ ion via selective fragmentation C-terminal to the aspartic acid residue, while GAILM(O)GAILR fragments almost exclusively by the loss of methane sulfenic acid (CH_3SOH, 64 Da). These preferential bond cleavages prevent the formation of "sequence" ions, thereby hindering the identification of these peptides. In contrast, under mobile proton conditions, protonated GAILDGAILA and GAILM(O)GAILA fragment via nonselective formation of sequence ions. Peptide ions with a partially mobile proton (GAILDGAILK and GAILM(O)GAILK) represent an intermediate case, with some selective dissociation occurring. Thus protonated GAILDGAILK yields an abundant $\mathbf{y}_5$ ion together with other sequence ions, while protonated GAILM(O)GAILK gives abundant CH_3SOH loss in conjunction with the formation of $\mathbf{b}_n$, $\mathbf{b}_n$-CH_3SOH, and $\mathbf{b}_n$-CH_3SOH-H_2O sequence ions. The observation of $\mathbf{b}_n$-CH_3SOH, and $\mathbf{b}_n$-CH_3SOH-H_2O sequence ions highlights the fact that partial sequestration of the ionizing proton not only affects the initial proton mobility during dissociation of the $[M + H]^+$ ion, but can also influence the subsequent fragmentation of the $[M + H - CH_3SOH]^+$ ion.

Second, RRKM modeling of time- and energy-resolved survival curves (SCs) reveal that selective cleavage due to methionine sulfoxide and aspartic acid residues are characterized by a large difference in dissociation dynamics; i.e., the Arrhenius pre-exponential factor (*A*) of peptide fragmentation via selective bond cleavage is 1−2 orders of magnitude lower than nonselective peptide bond cleavage, while the dissociation threshold (E_0)

is relatively invariant. Thus selective bond cleavage is kinetically disfavored compared to nonselective amide bond cleavage.

Another key observation is that the energetics and dynamics of preferential loss of CH_3SOH from peptide ions containing methionine sulfoxide are very similar to selective C-terminal amide bond cleavage to aspartic acid residue. Interestingly, the fragmentation of protonated peptides occurring under partial proton mobility is characterized by fragmentation dynamics similar to those occurring under nonmobile proton conditions. These results suggest that while preferential cleavage can compete with amide bond cleavage energetically, dynamically, these processes are much slower compared to amide bond cleavage, explaining why these selective bond cleavages are not observed if fragmentation is performed under mobile proton conditions. This study also highlights the importance of entropic effects in the gas-phase fragmentation of peptide ions.

The SID FT-ICR MS approach has yet again proven to provide valuable information on the energetics and dynamics of important fragmentation processes. Given the large number of other reactive residues in a peptide, other selective bond cleavage reactions are also possible,[10] and these can potentially be examined using time- and energy-resolved studies. Indeed, this approach is currently being used to study the energetics and dynamics of other types of reactions, including electron and proton transfer[27] and peptide−antibiotic interaction.[28]

Acknowledgment. We thank ARC for financial support via Grant DP0558430 (to R.A.J.O.) and the ARC Centre of Excellence in Free Radical Chemistry and Biotechnology. H.L. acknowledges the award of the Elizabeth and Vernon Puzey Postgraduate Scholarship and the John and Allan Gilmour Research Awards. The experimental work described in this paper was performed at the W. R. Wiley Environmental Molecular Sciences Laboratory (EMSL), a national scientific user facility sponsored by the U.S. Department of Energy's Office of Biological and Environmental Research and located at Pacific Northwest National Laboratory (PNNL). PNNL is operated by Battelle for the U.S. Department of Energy. J.L. acknowledges the support from the Chemical Sciences Division, Office of Basic Energy Sciences of the U.S. Department of Energy.

References and Notes

(1) Mann, M.; Jensen, O. N. Proteomic analysis of post-translational modifications. *Nat. Biotechnol.* **2003**, *21*, 255−261.

(2) Jensen, O. N. Modification-specific proteomics: characterization of post-translational modifications by mass spectrometry. *Curr. Opin. Chem. Biol.* **2004**, *8*, 33−41.

(3) Reid, G. E.; Roberts, K. D.; Kapp, E. A.; Simpson, R. J. Statistical and Mechanistic Approaches to Understanding the Gas-Phase Fragmentation Behavior of Methionine Sulfoxide Containing Peptides. *J. Proteome Res.* **2004**, *3*, 751−759.

(4) Wysocki, V. H.; Tsaprailis, G.; Smith, L. L.; Breci, L. A. Mobile and localized protons: a framework for understanding peptide dissociation. *J. Mass Spectrom.* **2000**, *35*, 1399−1406.

(5) Paizs, B.; Suhai, S. Fragmentation pathways of protonated peptides. *Mass Spectrom. Rev.* **2005**, *24*, 508−548.

(6) Tsaprailis, G.; Nair, H.; Somogyi, A.; Wysocki, V. H.; Zhong, W.; Futrell, J. H.; Summerfield, S. G.; Gaskell, S. J. Influence of Secondary Structure on the Fragmentation of Protonated Peptides. *J. Am. Chem. Soc.* **1999**, *121*, 5142−5154.

(7) Wang, Y.; Vivekananda, S.; Men, L.; Zhang, Q. Fragmentation of Protonated Ions of Peptides Containing Cysteine, Cysteine Sulfinic Acid, and Cysteine Sulfonic Acid. *J. Am. Soc. Mass Spectrom.* **2004**, *15*, 697−702.

(8) Men, L.; Wang, Y. Further studies on the fragmentation of protonated ions of peptides containing aspartic acid, glutamic acid, cysteine sulfinic acid, and cysteine sulfonic acid. *Rapid Commun. Mass Spectrom.* **2005**, *19*, 23−30.

(9) Chowdhury, S. M.; Munske, G. R.; Ronald, R. C.; Bruce, J. E. Evaluation of Low Energy CID and ECD Fragmentation Behavior of Mono-Oxidized Thio-Ether Bonds in Peptides. *J. Am. Soc. Mass Spectrom.* **2007**, *18*, 493−501.

(10) Lioe, H.; O'Hair, R. A. J. A Novel Salt Bridge Mechanism Highlights the Need for Non-Mobile Proton Conditions to Promote Disulfide Bond Cleavage in Protonated Peptides under Low-Energy Collisional Activation. *J. Am. Soc. Mass Spectrom.* **2007**, *18*, 1109−1123.

(11) O'Hair, R. A. J.; Reid, G. E. Neighboring group versus *cis*-elimination mechanisms for side chain loss from protonated methionine, methionine sulfoxide and their peptides. *Eur. J. Mass Spectrom.* **1999**, *5*, 325−334.

(12) Lioe, H.; O'Hair, R. A. J.; Gronert, S.; Austin, A.; Reid, G. E. Experimental and theoretical proton affinities of Methionine, Methionine sulfoxide and their N- and C-terminal derivatives. *Int. J. Mass Spectrom.* **2007**, in press.

(13) Lee, S.-W.; Kim, H. S.; Beauchamp, J. L. Salt Bridge Chemistry Applied to Gas-Phase Peptide Sequencing: Selective Fragmentation of Sodiated Gas-Phase Peptide Ions Adjacent to Aspartic Acid Residues. *J. Am. Chem. Soc.* **1998**, *120*, 3188−3195.

(14) Summerfield, S. G.; Whiting, A.; Gaskell, S. J. Intra-ionic interactions in electrosprayed peptide ions. *Int. J. Mass Spectrom. Ion Processes* **1997**, *162*, 149−161.

(15) Bailey, T. H.; Laskin, J.; Futrell, J. H. Energetics of selective cleavage at acidic residues studied by time- and energy-resolved surface-induced dissociation in FT-ICR MS. *Int. J. Mass Spectrom.* **2003**, *222*, 313−327.

(16) Laskin, J.; Bailey, T. H.; Futrell, J. H. Fragmentation energetics for angiotensin II and its analogs from time- and energy-resolved surface-induced dissociation studies. *Int. J. Mass Spectrom.* **2004**, *234*, 89−99.

(17) Laskin, J.; Denisov, E. V.; Shukla, A. K.; Barlow, S. E.; Futrell, J. H. Surface-induced dissociation in a Fourier transform ion cyclotron resonance mass spectrometer: Instrument design and evaluation. *Anal. Chem.* **2002**, *74*, 3255−3261.

(18) Shaffer, S. A.; Tang, K.; Anderson, G. A.; Prior, D. C.; Udseth, H. R.; Smith, R. D. A novel ion funnel for focusing ions at elevated pressure using electrospray ionization mass spectrometry. *Rapid Commun. Mass Spectrom.* **1997**, *11*, 1813−1817.

(19) Senko, M. W.; Canterbury, J. D.; Guan, S.; Marshall, A. G. A High-performance Modular Data System for Fourier Transform Ion Cyclotron Resonance Mass Spectrometry. *Rapid Commun. Mass Spectrom.* **1996**, *10*, 1839−1844.

(20) Laskin, J.; Byrd, M.; Futrell, J. Internal energy distributions resulting from sustained off-resonance excitation in FTMS. I. Fragmentation of the bromobenzene radical cation. *Int. J. Mass Spectrom.* **2000**, *195/196*, 285−302.

(21) Laskin, J.; Futrell, J. Internal Energy Distributions Resulting from Sustained Off-Resonance Excitation in Fourier Transform Ion Cyclotron Resonance Mass Spectrometry. II. Fragmentation of the 1-Bromonaphthalene Radical Cation. *J. Phys. Chem. A* **2000**, *104*, 5484−5494.

(22) Laskin, J.; Bailey, T. H.; Futrell, J. H. Shattering of peptide ions on self-assembled monolayer surfaces. *J. Am. Chem. Soc.* **2003**, *125*, 1625−1632.

(23) Derrick, P. J.; Lloyd, P. M.; Christie, J. R. Physical chemistry of ion reactions. In *Advances in Mass Spectrometry*; Cornides, I., Howárth, G., Vékey, K., Eds.; Wiley: Chichester, 1995; pp 23−52.

(24) Lagerwerf, F. M.; van de Weert, M.; Heerma, W.; Haverkamp, J. Identification of oxidized methionine in peptides. *Rapid Commun. Mass Spectrom.* **1996**, *10*, 1905−1910.

(25) Laskin, J., Energy and Entropy Effects in Gas-Phase Dissociation of Peptides and Proteins. In *Principles of Mass Spectrometry Applied to Biomolecules*; Laskin, J., Lifshitz, C., Eds.; John Wiley and Sons: New York, 2006.

(26) Lifshitz, C. Kinetic shifts. *Eur. J. Mass Spectrom.* **2002**, *8*, 85−98.

(27) Laskin, J.; Yang, Z.; Lam, C.; Chu, I. Energetics and Dynamics of Electron Transfer and Proton Transfer in Dissociation of $Metal^{III}$(salen)-Peptide Complexes in the Gas-Phase. Presented at the 55th American Society for Mass Spectrometry (ASMS) Conference, 2007.

(28) Yang, Z.; Laskin, J. Experimental and Theoretical Studies of the Structures and Interactions of Vancomycin Antibiotics with Cell Wall Analogues Peptides. Presented at the 55th American Society for Mass Spectrometry (ASMS) Conference, 2007.